Is the zero Reynolds number approximation valid for ciliary flows?

Wei, Da; Dehnavi, Parviz Ghoddoosi; Aubin-Tam, Marie Eve; Tam, Daniel

DOI
10.1103/PhysRevLett.122.124502

Publication date
2019

Document Version
Final published version

Published in
Physical Review Letters

Is the Zero Reynolds Number Approximation Valid for Ciliary Flows?

Da Wei,[1] Parviz Ghoddoosi Dehnavi,[2] Marie-Eve Aubin-Tam,[1,*] and Daniel Tam[2,†]
[1]Department of Bionanoscience, Delft University of Technology, 2628CJ Delft, Netherlands
[2]Laboratory for Aero and Hydrodynamics, Delft University of Technology, 2628CD Delft, Netherlands

(Received 3 July 2018; revised manuscript received 8 January 2019; published 28 March 2019)

Stokes equations are commonly used to model the hydrodynamic flow around cilia on the micron scale. The validity of the zero Reynolds number approximation is investigated experimentally with a flow velocimetry approach based on optical tweezers, which allows the measurement of periodic flows with high spatial and temporal resolution. We find that beating cilia generate a flow, which fundamentally differs from the stokeslet field predicted by Stokes equations. In particular, the flow velocity spatially decays at a faster rate and is gradually phase delayed at increasing distances from the cilia. This indicates that the quasisteady approximation and use of Stokes equations for unsteady ciliary flow are not always justified and the finite timescale for vorticity diffusion cannot be neglected. Our results have significant implications in studies of synchronization and collective dynamics of microswimmers.

DOI: 10.1103/PhysRevLett.122.124502

Cilia and flagella are organelles essential for motility that extend from eukaryotic cells. For eukaryotic organisms, these organelles are the generic solution to the physical challenges posed by pumping fluids and generating propulsion, on the viscosity-dominated micron scale [1]. To generate flow fields, cilia actively bend in periodic power-recovery strokes and interact with the surrounding fluid [2,3]. Modeling the hydrodynamics around cilia is of high interest, and is central to studies of single cell locomotion [4–7], synchronization of cilia in metachronal waves [8–14], and interactions and collective motion between microswimmers [15,16].

On the micron scales, flow is dominated by viscosity, and the Reynolds number $\mathrm{Re} = \rho U l/\mu$ is small. Here, ρ denotes density, μ kinematic viscosity, l and U the characteristic length and velocity scale. In this regime, the equations governing the hydrodynamics are commonly approximated by Stokes equations, corresponding to the limit of zero Re

$$\nabla \cdot u = 0, \qquad -\nabla p + \mu \nabla^2 \mathbf{u} = \mathbf{0}, \tag{1}$$

where $\mathbf{u}$ and p are velocity and pressure fields [17]. Equation (1) is a simplification of Navier-Stokes equations, in the limit when vorticity instantly diffuses to infinity and the viscous boundary layer extends to the entire fluid domain. One fundamental solution to Eq. (1) is the stokeslet, which represents the flow induced by a point force and whose velocity field decays in $1/r$. The stokeslet is the cornerstone of theoretical models in microhydrodynamics and is relevant to established numerical methods, e.g., the boundary element method (BEM) [18] or the method of regularized stokeslet [19], as well as reduced models representing the flow around cilia and microswimmers [7,20]. Time varying stokeslets have been used to represent the periodic motion of hydrodynamically coupled oscillators and elucidate the emergence of synchronization and metachronal waves in cilia [8–10,21]. However, unsteady flows induced by cilia are characterized by Reynolds numbers, which, though small, are not zero. This has implications for the motility of microorganisms and synchronization [6,22]. This study investigates the validity of the stokeslet approximation with experimental velocimetry measurements. Such direct experimental measurements of time varying flows are challenging owing to the high frequency of the ciliary motion $f = 10$–100 Hz. Previous quantitative measurements of the velocity decay around cilia have been limited to average flow velocities [20,23].

Here, we use optical tweezers-based velocimetry (OTV) [24,25] to measure unsteady flows around a cilium. We find the flow to differ fundamentally from the flow predicted in the zero Re regime. First, the rate of spatial decay of the velocity is much higher, thereby limiting the range of hydrodynamic interactions. In addition, we evidence an important phase delay of the oscillatory velocity component, which gradually leads to flow inversion away from the cilium. Our experimental results highlight the limitations of using stokeslets to represent unsteady flows and in particular for studies of synchronization in cilia and microswimmers.

In our OTV method, we directly measure the hydrodynamic force exerted on a microbead to determine the flow velocity [24,25]. The optical tweezers setup is similar to Ref. [26]. A laser beam ($\lambda = 1064$ nm) is focused through a water immersion objective (Nikon CFI PlanApo VC 60X NA = 1.20). Around the laser focal point, beads present in solution are subject to a trapping

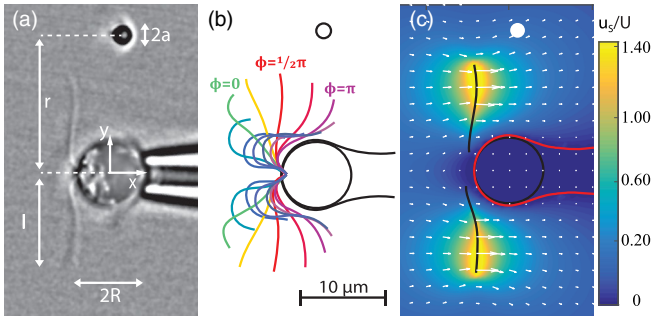

FIG. 1. (a) An optically trapped bead measures the local flow around the cilia of a *Chlamydomonas reinhardtii* cell held by a micropipette. (b) Tracked flagellar shapes from image analysis of a video-recorded beating cycle. (c) Flow velocity field corresponding to the cell in (a), computed by solving Stokes equations.

force $\mathbf{F} = -k\Delta\mathbf{x}$, where $\Delta\mathbf{x}$, the bead displacement from the laser beam focus, is monitored with back focal plane interferometry with high temporal resolution (<0.1 ms). We use beads of radii $a = 1$–$2.5\ \mu$m and trap stiffnesses $k = 12$–$50\ \mathrm{pN}\,\mu\mathrm{m}^{-1}$.

At a given location, flow velocities $\mathbf{u}(t)$ are deduced from bead displacements $\mathbf{\Delta x}$. For unsteady flows, the dynamics of the trapped bead is governed by the Boussinesq-Basset-Oseen (BBO) equation. The particle Reynolds number $\mathrm{Re}_a = \rho|\mathbf{u}|a/\mu$ is small $\mathrm{Re}_a \approx 10^{-5} - 10^{-4}$ and the inertia, added mass, and Basset forces are negligible [17]. The BBO equation then reduces to a first order equation balancing the trapping force and the hydrodynamic drag

$$\dot{\mathbf{\Delta x}} + \frac{k}{\zeta}\Delta\mathbf{x} = \mathbf{u}(t), \tag{2}$$

which allows us to deduce the flow velocity $\mathbf{u}(t)$ from the displacement $\mathbf{\Delta x}$ [27].

The flow velocity $\mathbf{u} = (u, v)$ is measured around the beating cilia of single *C. reinhardtii* cells, held by suction with a glass pipette, at a height of 120 μm from the surface, following Ref. [28]. Cells varied in cell body radius $R = 4.4 \pm 0.8\ \mu$m, cilia length $l = 11.5 \pm 2.0\ \mu$m, and ciliary beating frequency $f = 53.0 \pm 5.0$ Hz. We measured the flow velocity using the OTV method at different positions from the cell center, in the xy plane of the cilia, where the x direction is aligned with the cell-pipette axis [Fig. 1(a)]. The flow induced by the cilia is notably larger in the x direction, and we report the velocity component u. We first focus on the velocity along the y axis for positions $(x = 0, y = r)$ at increasing lateral distances from the cell center $r \approx 20$–$120\ \mu$m. Figure 2 presents flow measurements for $r/l = 1.7$ and $r/l = 4.9$. Results are nondimensionalized with l, the length of the cilia, f the beating frequency, and $U = lf$, the typical cilia velocity. OTV measurements are synchronized with high-speed video recordings of the beating cilia using an sCMOS camera at a frame rate of 400–850 fps [Fig. 1(a)]. For each frame, we track the cilia shape and reconstruct periodic deformations [Fig. 1(b)]. The ciliary phase $\phi(t)$ is defined from a principal component analysis, similarly to [4], with the convention $\phi = 0$ when the cilia transition from the recovery to the power stroke and extend the furthest from the cell; see Fig. 1(b). To evaluate the validity of the zero Reynolds regime, we use the tracked ciliary deformations to compute the flow velocity fields predicted by Eq. (1). Stokes equations (1) are solved numerically using a hybrid BEM and slender-body approach, similar to [17]. The cell body and the glass pipette are represented with a completed double layer boundary integral equation, with the singularities of the completion flow distributed along the centerline of the pipette [29]. The cilia are represented using slender-body theory [30]. We use this computational

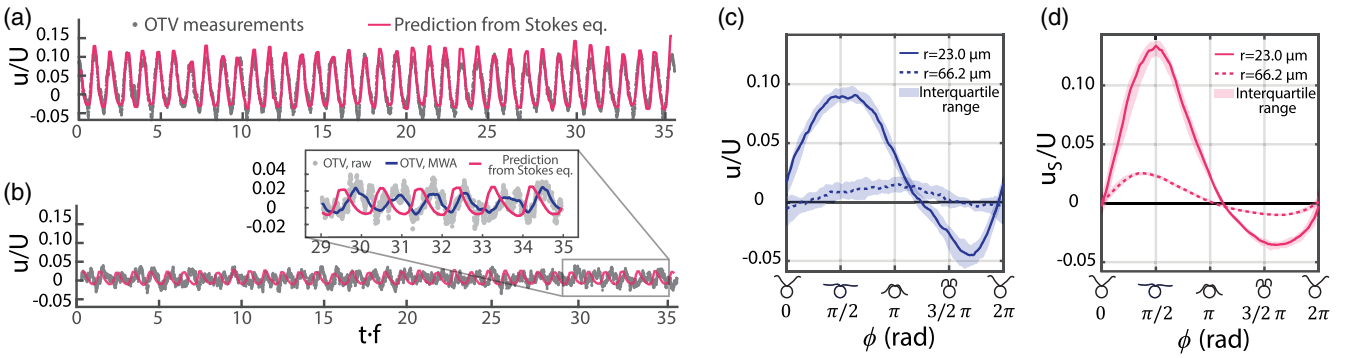

FIG. 2. Comparison between the flow velocity experimentally measured with OTV (gray) and the flow computed with BEM (magenta). (a) Close to the cell, $r = 23.0\ \mu$m, the measurements appear in phase. (b) At larger distances from the cell center, $r = 66.2\ \mu$m, the OTV measurements of the velocity is phase delayed compared to what is predicted from solving Stokes equations (inset) OTV raw data (gray), moving-window-averaged data (blue), and the flow computed with BEM (magenta). (c)–(d) Flow velocity u over one period, averaged for ~40 periods, for the OTV measurements (c) compared to u_S calculated with BEM from the tracked shapes (d). Solid and dashed lines correspond to the velocity at $r = 23.0\ \mu$m and $r = 66.2\ \mu$m, respectively. A beat cycle begins when the cilia reach the most forward position, at the start of the power stroke. The flow velocity predicted by Stokes equations is in phase at different distances from the cell (d), whereas it is phase delayed in our OTV measurements (c).

approach to compare OTV velocity measurements $\mathbf{u}(t)$ with the flow velocity field predicted by Stokes equations $\mathbf{u}_S$; see Fig. 1(c).

Figure 2 represents OTV measurements of u as a function of time compared with flow velocities predicted from solving Stokes equations u_S for tracked ciliary deformations. Close to the cilia, for $r/l = 1.7$, velocity measurements are in quantitative agreement with the solution to Stokes equations. In particular, on Fig. 2(a), measurements capture the high frequency periodicity of the ciliary flow, with positive flow velocities $u(y,t)$ caused by the power stroke and negative flow velocities by the recovery stroke. A few cilia length away from the cell, flow measurements show significant discrepancies with Stokes flow. Figure 2(b) represents our flow measurements at $y/l = 4.9$. At these distances, the periodicity of the ciliary flow can still be clearly seen from the raw data and the amplitude of flow oscillations is reduced as expected for Stokes flow. However, OTV measurements reveal a phase shift in the flow velocity u, which the solution u_S to Stokes equations does not predict; see Fig. 2(b). This phase shift θ is estimated from computing the cross-correlation between $u(t)$ and $u_S(t)$. The time shift in Fig. 2(b) is ≈3.7 ms corresponding to a phase shift of $\theta \approx 3\pi/8$ at $r/l \approx 4.9$. The velocity oscillations generated by the power-recovery strokes become gradually phase delayed as the distance to the cell increases [Fig. 2(c)]. Close to the cell, u reaches a maximum in the middle of the power stroke, for $\phi \approx \pi/2$, as predicted by Stokes equations, whereas 4.9 ciliary length away, u reaches its maximum later in the stroke, toward the beginning of the recovery stroke, when $\phi \approx \pi$; see Fig. 2(c). Hence, the velocity magnitude at $r/l \approx 4.9$ reaches a maximum when the velocity magnitude close to the cell (at $r/l \approx 1.7$) is minimum and equal to zero. Therefore, the flow fundamentally differs from the flow u_S, expected in the zero Re limit, where the flow is in-phase at all distances; see Fig. 2(d).

We further investigate the spatial decay in flow velocity at increasing distances r from the cell (Fig. 3). We first consider u_S predicted from solving Stokes equations. At a given phase ϕ during the stroke, u_S has the same sign at all locations along the y axis and oscillates between being positive at all r during the power stroke and being negative everywhere during the recovery stroke; see Fig. 3(a). This is because Stokes equations assume the instantaneous diffusion of vorticity and momentum to infinity. The direction of Stokes flow in an unbounded domain always follows the direction of the forcing in the entire fluid domain. In contrast, our measurements of u reveal flow inversion, where the flow direction changes at increasing distances from the cell. The sign of u only agrees with the numerical solution to Stokes equation in the cell vicinity and is the opposite far away; see Fig. 3(a) and 3(b). For example, when $\phi \approx \pi/10$, the cilia are at the beginning of the power stroke, u is positive close to the cell, but negative

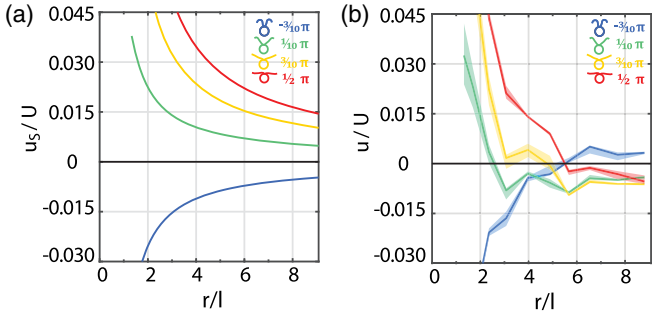

FIG. 3. Flow velocity as a function of the distance to the cell center at separate ciliary phases (a) corresponds to the flow computed with the BEM from the tracked shapes and (b) to the OTV measurements. (a),(b) Velocity profiles are represented at the same stages during the power-recovery strokes. Each color represents different ciliary phases, ϕ, as indicated in the legend. OTV measurements (b) reveal the existence of an inversion point, where the direction of the flow reverses, which is not predicted by the BEM computation.

beyond an inversion point when $r/l \geq 2.7$. The inversion point, for which $u = 0$, moves away from the cell as the ciliary phase ϕ increases, and reaches $r/l = 5.6$, in the middle of the power stroke, when $\phi \approx \pi/2$ and u is maximum close to the cell. At the beginning of the recovery stroke, when the cilia reverts the direction of its motion, another inversion point is created near the cell and later propagates away from the cell; see Fig. 3(b). The instantaneous velocity distribution is markedly different from Stokes predictions throughout the beating cycle and differences appear as close as $r/l \sim 2$–3; see the Supplemental Material [31] representing the flow field over the entire beat compared with Stokes flow.

The experimental results in Figs. 2 and 3 are reminiscent of Stokes' second problem and point toward the breakdown of the quasisteady approximation of Stokes flows [31]. The OTV allows us to resolve the finite time required for the vorticity created at the surface of the organism to diffuse to the bulk. Although commonly neglected, the effect of the unsteady term of Navier-Stokes equations in microhydrodynamics is well known [6,17,32]. Theoretically, the solution to unsteady Stokes equations for an oscillating point force prototypically shows how small Re alter the zero Re solution [17]. In this case, the relevant length scale is $\delta = \sqrt{\mu/\rho f}$, the characteristic length scale of vorticity diffusion $\delta \approx 130$ μm. At short distances from the point force $r \ll \delta$, the transient associated with the diffusion of vorticity is very short and the solution tends to the stokeslet. For large distances r, the spatial decay of the flow velocity becomes significantly stronger than for the stokeslet and scales with $1/r^3$ [17]. In addition, flow oscillations are predicted to be phase delayed with the forcing. It is interesting to then decompose velocity measurements as $u(y,t) = \bar{u}(y) + u'(y,t)$, where $\bar{u}(y)$ is the average flow and $u'(y,t)$ are the zero-averaged oscillations. We further

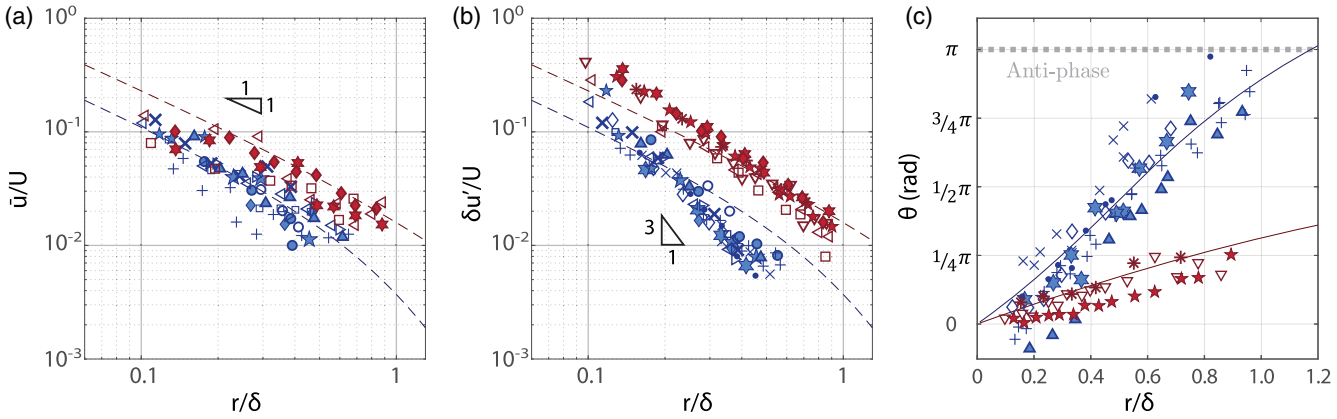

FIG. 4. Characteristics of the flow measured with the OTV as a function of r/δ. Different symbols represent datasets for different cells, with beads of 1 μm (open symbols) or 2.5 μm (other symbols) radii. Measurements are taken along the y axis (blue) at positions $(x = 0, r)$ and along the x axis (red) at positions $(r, y = 0)$. We report the average flow velocity $\bar{u}$ (a) and the amplitude of the zero-averaged oscillatory component $\delta u'$ (b). Dashed lines show predictions from Stokes equations for a point force located 120 μm above a solid surface. The decay rate of the oscillatory flow $\delta u'$ ($\sim 1/r^3$) is faster compared to the decay rate of the average flow $\bar{u}$ ($\sim 1/r$). (c) Phase shift θ between the experimental and the computed results. Solid lines show predictions from the unsteady Stokes equations for an oscillating point force.

denote $\delta u'(y)$ the amplitudes of the flow oscillations u'. In the limit of zero Re, $\bar{u}$ and $\delta u'$ are expected to both follow the same $1/r$ rate of decay as the stokeslet. However, from linearity, one would expect very different rates of spatial decay for the average flow $\bar{u}$ and the oscillations $\delta u'$, if transient effects are important. Figure 4 represents the velocity field measured for several different cells. $\bar{u}$ is obtained directly by computing the average velocity over the entire duration of the experiment and $\delta u'$ is the average amplitude of u'. The rate of spatial decay of $\bar{u}$ and $\delta u'$ is different and can be compared to the rate of velocity decay expected from the solution to Stokes equations for a point force located 120 μm from a solid wall [Figs. 4(a) and 4(b)]. $\bar{u}$ follows the decay in $1/r$ expected from the stokeslet solution [Fig. 4(a)]. On the other hand, the rate of decay of $\delta u'$ is different and we find $\delta u'$ to decay faster than $1/r$, expected from Eq. (1), and closer to $1/r^3$ predicted by the unsteady Stokes equations [Fig. 4(b)]. We now consider the phase delay θ between the cilium and the oscillatory flow u'. We find the phase delay to increase with distance from $\theta = 0$ (in-phase) to $\theta \approx \pi$ (antiphase); see Fig. 4(c) (blue symbols). At a distance $r \approx \delta$, which can be regarded as the boundary layer thickness, the flow is in antiphase with the cilium, which quantitatively agrees with the flow predicted from the unsteady Stokes equations for an oscillating point force [17] [Fig. 4(c)]. The slope in Fig. 4(c) (blue symbols) corresponds to a phase increase of $\sim 0.032 \pm 0.003$ rad μm^{-1} and hence to a $\sim \pi/2$ phase increase over a distance of ~ 50 μm. In addition, we performed measurements of u at increasing positions along the x axis (Fig. 4, red symbols). Similar to the stokeslet field around a point force in the x direction, u is larger along the x axis compared to the y axis; see Figs. 4(a) and 4(b). Along the y axis, we find similar trends as along the x axis: the rate of decay of the average flow agrees with predictions from Stokes equations [Fig. 4(a)] while the oscillatory component decays faster. Furthermore, we find the phase increase of the x component of the velocity to be lower along the x axis then along the y axis. This agrees with the solution to the unsteady Stokes equations for an oscillating point force along the x axis [Fig. 4(c), solid lines]. This solution is axisymmetric about the x axis and the phase increase depends on the direction: it is minimum in the direction of the oscillating force, the x axis, in agreement with our measurements, and is maximum in any direction perpendicular to the x axis, in agreement with our measurements along the y axis. Though not measured experimentally, the phase increase along the z axis is expected, from the axisymmetry of the solution, to be similar to the reported y-axis measurements.

In this Letter, we present direct experimental evidence of the shortcomings of using Stokes equations to represent micron scale flows generated by beating cilia and flagella. We find the amplitude of the oscillatory flow velocity to decay much faster than the average flow and the oscillations of the flow velocity to be gradually phase shifted at increasing r. Although the zero Reynolds number limit is justified to model hydrodynamic forces on cilia for motility studies, it does not accurately predict the range and nature of hydrodynamic interactions, for oscillatory flows relevant to synchronization. The discrepancies in amplitude and phase are not limited to the far field, for $r \gg \delta$ beyond the diffusive length scale. Instead, significant differences between our measurements and Stokes predictions already appear at surprisingly short distances from the cell of $r \approx 2$–$3l$. The inaccuracy of the zero Reynolds number approximation originates in the quasisteady approximation, which fails to take into account the diffusive timescale of

vorticity. Our experimental observations are general and characteristic of how the unsteady term in the Navier-Stokes equations affects the flow, and will be present in other flow configurations, e.g., for cilia close to a no-slip wall. For such a point force close to a wall, the decay of the velocity field will increase from $1/r^3$, for the quasisteady approximation given by the Blake tensor, to $1/r^5$. Our results have implications in studies of hydrodynamic synchronization between cilia and flagellated microswimmers.

The authors thank R. Kieffer for technical support and acknowledge a stimulating conversation with B. Eckhardt. The work was supported by the H2020 European Research Counsil (Grant agreement No. 716712) and the Netherlands Organization for Scientific Research (Frontiers of Nanoscience program).

*m.e.aubin-tam@tudelft.nl
†d.s.w.tam@tudelft.nl

[1] E. Lauga and T. R. Powers, Rep. Prog. Phys. **72**, 096601 (2009).
[2] R. Golestanian, J. M. Yeomans, and N. Uchida, Soft Matter **7**, 3074 (2011).
[3] J. Elgeti, R. G. Winkler, and G. Gompper, Rep. Prog. Phys. **78**, 056601 (2015).
[4] V. F. Geyer, F. Jülicher, J. Howard, and B. M. Friedrich, Proc. Natl. Acad. Sci. U.S.A. **110**, 18058 (2013).
[5] R. R. Bennett and R. Golestanian, Phys. Rev. Lett. **110**, 148102 (2013).
[6] G. S. Klindt and B. M. Friedrich, Phys. Rev. E **92**, 063019 (2015).
[7] K. Ishimoto, H. Gadêlha, E. A. Gaffney, D. J. Smith, and J. Kirkman-Brown, Phys. Rev. Lett. **118**, 124501 (2017).
[8] B. Guirao and J.-F. Joanny, Biophys. J. **92**, 1900 (2007).
[9] A. Vilfan and F. Jülicher, Phys. Rev. Lett. **96**, 058102 (2006).
[10] T. Niedermayer, B. Eckhardt, and P. Lenz, Chaos **18**, 037128 (2008).
[11] N. Uchida and R. Golestanian, Phys. Rev. Lett. **104**, 178103 (2010).
[12] J. Elgeti and G. Gompper, Proc. Natl. Acad. Sci. U.S.A. **110**, 4470 (2013).
[13] D. R. Brumley, M. Polin, T. J. Pedley, and R. E. Goldstein, Phys. Rev. Lett. **109**, 268102 (2012).
[14] D. R. Brumley, K. Y. Wan, M. Polin, and R. E. Goldstein, eLife **3**, e02750 (2014).
[15] C. M. Pooley, G. P. Alexander, and J. M. Yeomans, Phys. Rev. Lett. **99**, 228103 (2007).
[16] G. J. Elfring and E. Lauga, J. Fluid Mech. **674**, 163 (2011).
[17] S. Kim and S. J. Karrila, *Microhydrodynamics: Principles and Selected Applications* (Courier Corporation, North Chelmsford, 2013).
[18] C. Pozrikidis, *A Practical Guide to Boundary Element Methods with the Software Library BEMLIB* (CRC Press, Boca Raton, FL, 2002).
[19] R. Cortez, SIAM J. Sci. Comput. **23**, 1204 (2001).
[20] K. Drescher, R. E. Goldstein, N. Michel, M. Polin, and I. Tuval, Phys. Rev. Lett. **105**, 168101 (2010).
[21] A. Maestro, N. Bruot, J. Kotar, N. Uchida, R. Golestanian, and P. Cicuta, Commun. Phys. **1**, 28 (2018).
[22] M. Theers and R. G. Winkler, Phys. Rev. E **88**, 023012 (2013).
[23] J. S. Guasto, K. A. Johnson, and J. P. Gollub, Phys. Rev. Lett. **105**, 168102 (2010).
[24] P. Almendarez-Rangel, B. Morales-Cruzado, E. Sarmiento-Gomez, R. Romero-Meendez, and F. G. Perez-Gutierrez, Eur. J. Mech. B **72**, 561 (2018).
[25] G. Knoner, S. Parkin, N. R. Heckenberg, and H. Rubinsztein-Dunlop, Phys. Rev. E **72**, 031507 (2005).
[26] M. J. Lang, C. L. Asbury, J. W. Shaevitz, and S. M. Block, Biophys. J. **83**, 491 (2002).
[27] M.-T. Wei, O. Latinovic, L. A. Hough, Y.-Q. Chen, H. D. Ou-Yang, and A. Chiou, in *Handbook of Photonics for Biomedical Engineering*, edited by A. P. Ho, D. Kim, and M. Somekh (Springer, Dordrecht, 2017), pp. 731–753.
[28] G. Quaranta, M.-E. Aubin-Tam, and D. Tam, Phys. Rev. Lett. **115**, 238101 (2015).
[29] E. E. Keaveny and M. J. Shelley, J. Comput. Phys. **230**, 2141 (2011).
[30] J. B. Keller and S. I. Rubinow, J. Fluid Mech. **75**, 705 (1976).
[31] See Supplemental Material at http://link.aps.org/supplemental/10.1103/PhysRevLett.122.124502 for a video comparing the instantaneous velocity distribution measured along the y axis throughout the beating cycle and compared with predictions from solving Stokes equations.
[32] S. Wang and A. Ardekani, J. Fluid Mech. **702**, 286 (2012).